Performance Analysis and Modeling of Graphene based On-chip Interconnects

Synopsis of the Thesis to be submitted in Partial Fulfillment
of the Requirements for the Award of the Degree of

Doctor of Philosophy

by

Vijay Rao Kumbhare
(Roll No: 175010102)

Under the Supervision of
Dr. Punya Prasanna Paltani
&
Dr. Manoj Kumar Majumder

Department of Electronics and Communication Engineering
International Institute of Information Technology, Naya Raipur
Raipur – 493661
June, 2021

International Institute of Information Technology Naya Raipur

Declaration by the Student

Date: 16-06-2021

Title of the Thesis: **Performance Analysis and Modeling of Graphene based On-chip Interconnects**

I Certify that

a. the work contained in the thesis is original and has been done by me under the guidance of my Supervisors;

b. the work has not been submitted to any other Institute for any degree or diploma;

c. I have followed the guidelines provided by the Institute in preparing the thesis;

d. I have conformed to ethical norms and guidelines while writing the thesis and;

e. whenever I have used materials (data, models, figures, and text) from other sources, I have given due credit to them by citing them in the text of the thesis, giving their details in the references, and taking permission from the copyright owners of the sources, whenever necessary.

Signature of the Student: Vijay

Name of the Student: **Vijay Rao Kumbhare (Roll No. 175010102)**

डॉ.श्यामाप्रसाद मुखर्जी अंतरराष्ट्रीय सूचना प्रौद्योगिकी संस्थान
DR. SHYAMA PRASAD MUKHERJEE INTERNATIONAL
INSTITUTE OF INFORMATION TECHNOLOGY, NAYA RAIPUR
(A Joint Initiative of NTPC & Govt. of Chhattisgarh)

Email: iiitnr@iiitnr.ac.in
Tel: +91-771-2474040
Web: www.iiitnr.ac.in

Declaration by the Supervisors

This is to certify that the thesis entitled "**Performance Analysis and Modeling of Graphene based On-chip Interconnects**", submitted by **Vijay Rao Kumbhare (R.No. 175010102)** to International Institute of Information Technology, Naya Raipur, is a record of bonafide research work under our supervision and we consider it worthy of consideration for the Synopsis of the Thesis to be submitted in partial fulfillment of the requirements for the award of the degree of Doctor of Philosophy of the Institute.

Supervisor

Co-Supervisor

Date: 16-06-2021

Abstract

In recent years, graphene has been emerged as an alternative interconnect material to overcome the issues associated with copper (Cu). The modeling of interconnect is the primary objective to enhance the performance of on-chip interconnects at lower technology. In this regard, the graphene in the form of graphene nanoribbon (GNR) and carbon nanotube (CNT) is considered as a suitable material for interconnect application. This work considers different configurations of random distribution mixed CNT bundle (RMCB) and spatial arrangements (SMCB) having higher tube density. Based on higher tube density, an accurate interconnect model is demonstrated for different configurations of MCBs to reduce the crosstalk effect. It has been observed that the carbon nanotube field-effect transistor (CNTFET) driver based RMCB exhibits on an average 29.19% and 39.56% improved crosstalk delay and power dissipation, respectively as compared to SMCB configurations at 700 μm lengths. The analysis has been further extended for propagation delay and equivalent area demonstration with an identical structure of multi-walled CNT (MWCNT) bundle and multi-layered graphene nanoribbon (MLGNR) interconnects. Using an accurate *RLGC* model, the equivalent parasitic expressions are derived analytically that encouragingly possess a good agreement with the experimental data for interconnect dimensions of width (w = 32 nm), thickness (t = 32 nm), dielectric constant (ε_r = 2.2), and height from the ground surface (h_g = 76.8 nm). It is evident from the experimental results that further reduction in feature size primarily results in the cross-coupling capacitance that dominates the interconnect performance. In order to mitigate this coupling effect, the proposed work demonstrates different shielding techniques for the stability and crosstalk reliability issues. As a result, an improved crosstalk-induced delay and power dissipation of 59.36% and 96.82%, respectively is observed for active shielded side contact (SC)-MLGNR than a top contact (TC)-MLGNR at 32 nm technology. Depending on the improved performance, the SC-MLGNR is further explored to focus on the electronic properties of the zig-zag (zz) type. In this regard, a pristine zzMLGNR with different intercalated doped materials is used to extract the equivalent parasitics for accurate interconnect modeling. It is evident that the Li intercalated Ru-zzMLGNR-Ru possesses an improved delay by a factor of 6.25 times compared to pristine Ru-zzMLGNR-Ru based on-chip interconnects, respectively. Therefore, side contact doped zzMLGNR can be a suitable choice for the futuristic nano-interconnect application at advanced technology.

Keywords: Crosstalk, stability, electromigration, mixed carbon nanotube bundle (MCB), multi-layered graphene nanoribbon (MLGNR).

1. Introduction

In the past several years, interconnect on an integrated circuit (IC) plays a vital role in providing proper functionality, reliability, power efficiency, and fabrication yields. The attention towards the interconnect became the major factor that determines the system and chip-level electrical performance due to continuous reduction in the feature size of transistors [1]. At advanced technology, the mostly used interconnect material copper (Cu) suffers from lower stability and durability due to the hillock and void formation caused by electromigration at higher current density [2]. For instance, these limitations of Cu interconnect are technology-dependent and will be more and more severe for the future generation of VLSI chips. In order to mitigate these challenges, the researchers are inspired to discover an alternate emerging material that can confer longer reliability, better performance, and improved stability at lower technology. In this regard, several research groups claimed that graphene-based interconnects can be a better replacement of existing Cu for the emerging area of nano-interconnects [1-5]. Carbon nanotubes (CNTs) and graphene nanoribbons (GNRs) are primarily known as allotropes of carbon and consist of a number of graphene sheets in the rolled-up and planar directions, respectively. Particularly, CNT/GNR provides an extraordinary and unique thermal conductivity as high as 5800 W/m-K, a higher current carrying ability of 10^{14} A/m^2, and a longer mean free path (MFP) in the range of micrometer [1, 2]. Moreover, the higher current carrying capability increases the reliability of the materials as compared to Cu and aluminum (Al) due to lower electromigration effects. GNRs can be classified as single- (SLGNR) and multi-layered GNR (MLGNR) based on the number of graphene sheets. Moreover, MLGNR exhibits higher conductivity than SLGNR due to more number of conducting channels associated with each graphene layer. Additionally, the edge roughness has been observed in the MLGNR at lower dimensions that is responsible for degrading the material properties. Due to the immature fabrication process, higher cost, and requirement of high-resolution lithography to obtain the smooth edge MLGNR, the rough edge MLGNR is still preferred in the current scenario [1, 4, 5]. Moreover, the improvement in the electronic properties of pristine graphene is further required due to lower conductivity that can meet the current demand of cutting-edge technology at lower physical dimensions. In a similar line, CNT can be classified as single-walled CNT (SWCNT) and multi-walled CNT (MWCNT), depending on the number of rolled-up cylinders. Several experiments [2, 6-8] demonstrate a realistic mixed CNT bundle (MCB) approach that primarily consists of SWCNT and MWCNT in the bundle. Moreover, the randomly distributed CNT in a bundle is preferred instead of spatially arranged CNT in a bundle as per the fabrication house [7, 8]. The effective resistance of MCB is approximately three times lower than the SWCNT and MWCNT due to the higher packing density of MCB [8]. Additionally, the MCBs demonstrate several advantages such as 1) lower contact resistance, 2) negligible impact of inter-CNT coupling capacitance, and 3) straightforward fabrication process and potential benefit of improving the conduction channels [2, 6-8].

Previously, several research groups in [9, 10] considered a one-dimensional liquid theory model to measure the tunneling through CNT based nano-transmission line. The work is extended to model the parallel CNTs and reported that the nanowires in parallel combination could improve the interconnect performance than a single quantum wire [10]. Moreover, flat CNT array, dense CNT bundle, and sparse CNT bundle are modeled for global interconnects based on several assumptions on placing the CNTs in a bundle [11]. These assumptions compromise with the accuracy of the interconnect modeling while neglecting the significance of different diameters of CNTs. In this regard, diameter-dependent SWCNT in a bundle is demonstrated in [12], and the concept of the diameter-based conducting channel using a compact physical model for MWCNT in [13]. It has been reported that the MCB can provide better interconnect

performance due to lower capacitive impact [14]. Further, the hierarchy model of MCB has been proposed in [15] to analyze the interconnect delay and crosstalk effect. The work has been extended in [8] while considering the spatially arranged SWCNT and MWCNT in a bundle and neglected the significance of randomly distributed CNTs in a bundle. Furthermore, the comparative analysis of MLGNR and MWCNT has been presented without considering the identical interconnect structure, imperfect contact resistance, and inter-layer/inter-shell tunneling. Later, metal-interface contact resistance is discussed in [16] for interconnect modeling of MLGNR and MWCNT. It is reported that the metal-graphene interface is also the major hurdle that slows down the industry at the nano-scale regime. Several researchers have discussed about the contact resistance due to improper alignment of the metal-graphene interface, resulting in higher contact resistance [16-17]. In this regard, the experimental results demonstrated that the formation of side contact (SC) of MLGNR is more reliable as compared to top contact (TC) due to a 77% reduction in contact resistance using controlled plasma treatment [18]. On the other hand, advancement in technology primarily increases the interconnect density resulting in higher cross-coupling capacitance. The impact of crosstalk needs to critically address that leads to digital logic faults and malfunction on the performance due to unintentional signal on victim line. In this regard, shielding methodologies have been proposed in [19] to prevent the interconnect performance against electromagnetic interference (EMI) and crosstalk. Furthermore, it has been reported that a shielded MLGNR is more reliable in terms of crosstalk and stability at lower technology [19, 20]. Owing to its lower dimensions, a further improvement in the pristine graphene is reported due to several factors. These factors such as inter-sheet electron hopping, reduced carrier MFP due to edge scattering, and bandgap opening are responsible for limiting the conductivity of pristine zig-zag (zz)-MLGNR at lower physical dimension [21-23].

To address these challenges and technical gaps, this work considered graphene as emerging interconnect materials to improve the performance and modeling of interconnects. Based on the above state-of-the-art, the technical gaps are listed in the following section.

2. Problem Statements

With the advent of miniaturization, the demand for higher operating frequency, and higher performance requirements, several research groups [1-4] explored different materials and approached to overcome the problem that arises on conventional material at advanced technology node. Based on a detailed literature review in the area of interconnect, several methodology and modeling of interconnects are explored to reduce the impact of propagation delay, crosstalk, and power dissipation. The state-of-the-art literature [1-6, 10-14, 20-23] shows several challenges associated with the advancement of technology. Therefore, the point-wise technical research gaps are identified as given below:

2.1 Realistic nature of randomly distributed CNT in a bundle: The CNT based metallic interconnect can be a suitable choice to replace the existing Cu interconnects in cutting-edge technology. Particularly, CNT exhibits an extraordinary unique thermal conductivity and higher current carrying capability than Cu material. Several research groups in [1-2, 9-14] demonstrated the significance of the different structures of SWCNTs, MWCNTs, and mixed CNTs having various diameters in a bundle. The behavior of conductivity with a variation in the diameter is demonstrated in [11-13] and modeling is carried out for SWCNT and MWCNT interconnects using a compact physical model [14, 15]. Although, the fabrication has been progressed for a similar diameter of CNTs in a bundle, but the production of high-quality of CNTs is still a challenging task. Moreover, as per the fabrication house [4, 7, 8], a densely packed MWCNT bundle is hard to achieve due to: 1) the non-uniform growth of CNT bundles, 2) distributed CNT diameters, and 3) difficult to handle the position of an individual CNT at a desired location inside the bundle.

In reality, the growth of CNTs in a bundle consists of MWCNT and SWCNT that follows the Gaussian distribution depending on the process control. It is reported that the synthesization and the growth of CNTs using plasma-enhanced chemical vapor deposition (PECVD) produce a mixture of SWCNT and MWCNTs. However, the growth of a pure SWCNT or MWCNT in a bundle is a challenging task, hence MCB is preferred. Moreover, the effective resistance of MCB is approximately three times lower than SWCNT and MWCNT due to the higher packing density of MCB. Furthermore, the nature of growing the CNTs inside a bundle is purely random and follows the Gaussian distribution depending on the process control and synthesis condition. However, the placement of SWCNTs and MWCNTs of different diameters in a bundle plays a crucial role in determining the interconnect performance. Therefore, accurate modeling of the realistic nature of a randomly distributed MCB (RMCB) and spatially arranged MCB (SMCB) is required to reduce the crosstalk effect using a higher tube density. Further, the challenges due to non-identical structural analysis that leads to inaccurate modeling of interconnects are discussed in the next technical gap.

2.2 Non-identical structural modeling of MWCNT and MLGNR interconnect: The graphene can be considered as promising interconnect materials owing to their outstanding electrical, thermal, and chemical properties [1, 2]. The MWCNT and MLGNR are primarily preferred due to their overall sheet resistance reduces for more numbers of parallel shells (rolled up sheets) and layers (stacked planar sheets), respectively [20, 21]. In the recent past, several investigations of MWCNT, Cu, and MLGNR have been reported in [6-9, 18-23] while considering the non-identical structure modeling. Moreover, the parasitic expressions associated with the interconnect model are essential to validate for a good agreement with the experimental data. The planar structure of MLGNR motivates to consider for the next-generation interconnect materials. The MLGNR becomes the center for attraction due to the modest and controlled fabrication process compared to the complex process involved to grow the MWCNT in a bundle [24]. Moreover, as per the fabrication house [4, 7, 8], a densely packed MWCNT bundle is hard to achieve due to: 1) the non-uniform growth of CNT bundles, 2) distributed CNT diameters, and 3) difficult to handle the position of an individual CNT at a desired location inside the bundle. The most existing approach using non-identical structural modeling that demonstrates inaccurate interconnect performance leading to lower reliability and functionality of the system. Therefore, it is required to extend the analysis for propagation delay and equivalent area using an accurate identical structure of MWCNT bundle and MLGNR interconnect. It is also required to validate the equivalent parasitic expression with the experimental data to increase the accuracy of the interconnect model.

2.3 Shielding approach and impact of contact types on MLGNR interconnect: Miniaturization of technology and demand for high operating frequency leads to an increase in the interconnect density, higher packing density, and lower reliability of the system. In addition, the closer proximity of wire leads to an increase in cross-coupling capacitance. Therefore, the crosstalk effect needs to be critically addressed, leading to digital logic faults and malfunction on the performance. From the circuit analysis point of view, several eminent groups in [25, 26] demonstrated that the SC-MLGNR is more preferable than TC-MLGNR. This is due to the fact that the more number of conducting channels associated with SC-MLGNR leading to a reduction in the overall resistance. Further, it has been reported in [18] that the formation of SC is more reliable as compared to TC due to a 77% reduction in contact resistance using controlled plasma treatment. To overcome the challenges with the advancement of technology, the shielding approach can be a suitable choice to reduce the impact of the crosstalk effect. Therefore, the crosstalk reliability and relative stability are required to critically analyze for TC-and SC-MLGNR interconnect using active and passive shielding methodology.

2.4 Atomic-level structural analysis and impact of doping on MLGNR: In recent, MLGNR becomes the most acceptable emerging material for the futuristic nano-interconnect. The high current density, large carrier mobility, better immunity to electromigration, high electrical and thermal conductivity, and ballistic nature of graphene at lower dimensions especially below 8 nm, provides the solution to overcome the challenges faced by Cu interconnect [1, 2, 4, 5]. Owing to the experimental and theoretical studies, several research groups in [21-23, 27, 28] reported that the performance of pristine graphene can be further enhanced by altering the physical and chemical property of graphene while incorporating the intercalated doped material between the graphene layers. In realistic nature, several factors such as inter-sheet electron hopping, reduced carrier MFP due to edge scattering, and bandgap opening are responsible for limiting the conductivity of pristine zzMLGNR at lower physical dimension [23-30]. In order to overcome these challenges, improvement is further required in the performance of the pristine zzMLGNR interconnect. In this regard, atomic-level structural modification can be a suitable choice to manipulate the physical structure of pristine graphene while incorporating the doping materials for enhancing the electronic properties. Therefore, it is required to analyze the impact of different intercalated dielectric materials to improve the transmission of signal, current carrying capability and number of conducting channels for zzMLGNR that can be further utilized for interconnect modeling.

3. Motivation and Objective

Based on the state-of-the-art, there are several key factors associated with graphene. The graphene exhibits extraordinary unique electronic properties and straightforward fabrication due to its planar structure. The ballistic nature of electrons can be observed in graphene due to an effective electron MFP of several micrometers. The higher electron mobility and drift velocity have been observed in graphene that results in higher conductivity. Moreover, the higher current carrying capability increases the reliability of the materials as compared to Cu, and Al due to lower electromigration effects. Therefore, the unique properties of graphene motivate us to consider it for interconnect application.

Depending on the technical gaps identified in Section 2, this report primarily focuses on the following objectives

3.1 MCB interconnect modeling: This work focuses on the modeling of RMCB and SMCB interconnect at lower technology. In this regard, the three different SMCB and RMCB configurations are considered using higher tube density to reduce the impact of crosstalk under the active shielding technique. Firstly, the three different SMCB topologies are considered by placing an MWCNT having the outer diameter of 7.8 nm at the periphery along with the centrally located CNTs having a diameter of 1.68, 2.36, and 3.04 nm. Similarly, three different RMCB configurations are proposed with diameters ranging from 1.68 – 7.8 nm, 2.36 – 7.8 nm, and 3.04 – 7.8 nm that follow the Gaussian distribution. Using the above-mentioned SMCB and RMCB configurations, coupled driver-interconnect-load setup driven by resistive and CNTFET driver is considered at 10 nm technology. Further, the interconnect is represented by using a *Pi*-type electrical network. The reason behind this is that a *Pi*-model provides an improved delay performance of almost 29.1% and 6.5% compared to an equivalent *L* and *T*-type networks, respectively at global interconnects. The *pi*-network primarily represents an equivalent single conductor (ESC) model of SMCB and RMCB interconnects. Moreover, the impact of resistive and CNTFET drivers on shielded and unshielded coupled interconnects are demonstrated at lower technology.

3.2 Identical structure of MLGNR and Bundled MWCNT: In order to resolve the issue related to non-identical structural comparison of circular MWCNT with rectangular MLGNR, firstly, this work

considers a bundle MWCNT having an equivalent area of MLGNR. An equivalent *pi*-type multi-conductor transmission line (MTL) *RLGC* network is modeled depending on the interconnect structure. Further, the MTL circuit is simplified as ESC to diminish the computation effort. The equivalent parasitic expressions are validated against experimental data to evaluate the proposed model. Moreover, the finite-difference time-domain (FDTD) approach is considered to address the accuracy of the proposed *Pi*-model that is computationally more accurate over *L* or *T*-type networks. The FDTD approach is derived analytically and compared with the simulation results. Further, MLGNR and bundled MWCNT are used to analyze the propagation delay and equivalent area for different interconnect lengths.

3.3 Shielding and different contact types: This work is accomplished to protect from unintentional logic faults that lead to erroneous functionality, lower stability and crosstalk reliability issues due to closer proximity and higher density of interconnects. An MLGNR is modeled while considering the edge roughness, Fermi energy, and contact types to provide a real fabrication scenario. Further, different shielding methodologies and contact types are considered to counter the impact of crosstalk. In this regard, an accurate *pi*-based circuit network is proposed for shielded TC-and SC-MLGNR interconnects. In order to account the higher-order functions, the ABCD parameters are derived to analyze the stability of the proposed structures. Additionally, a unique *pi*-type network is taken into account for the proposed work that exhibits higher computational accuracy. Moreover, the different temperature variations are considered in order to identify the breakdown region for MLGNR material. Mean time to failure (MTTF) is used to address the reliability issues as compared with Cu at 32 nm technology. In order to have a smooth fabrication process and compatibility with CMOS technology, this work is considered a 32 nm technology. However, scaling the technology down to 32 nm produces several challenges, such as closer proximity of wire that is difficult to isolate from each other, and required high-resolution lithography along with the complex process.

3.4 Edge passivation and doping: In reality, the SC pristine MLGNR faces several issues such as lower conductivity due to crystalline defect, higher roughness, lower mobility that results from lower quality of graphene sheet. In this regard, this work focuses on improving the electronic properties of SC pristine MLGNR by incorporating the different intercalated doped materials such as Li, AsF_5, $FeCl_3$, and $MoCl_5$. Moreover, the significance of edged passivation is presented using hydrogen (H) and ruthenium (Ru) atoms at both sides of zzMLGNR edges to maintain the metallic behavior. Firstly, the band structure is analyzed for the validation of the metallic nature of zzMLGNR using energy-momentum relation. The proposed structure is optimized to obtain the maximum transmission of signal in the channel region. The optimized structure is used to extract the equivalent parasitics associated with the pristine and intercalated doped zzMLGNR. Using extracted equivalent parasitics, the proposed structure is modeled into an equivalent *pi*-type electrical network to analyze the propagation delay at lower dimensions.

4. Work done in the thesis

The performance and efficient modeling of interconnects have been presented using graphene as an emerging material. Each subsection starts with the problem statement, followed by modeling of interconnects. The results associated with each contribution are demonstrated at the end of each section.

4.1 Comparative analysis and modeling of RMCB and SMCB based interconnects[1]

Technology advancement limits the performance of Cu interconnects due to higher resistivity. The graphene has been emerged as an alternative interconnect material to overcome these challenges. The existing approach demonstrates better interconnect performance based on SWCNT and MWCNT. However, the modeling of pure SWCNT and MWCNT exhibits inaccurate interconnect performance. As per the fabrication house, the growth of CNT follows Gaussian distribution in reality and contains the different diameters of CNTs in a bundle. Therefore, the graphene based mixed carbon nanotube bundles (MCB) with RMCB and SMCB having higher tube density is considered to propose an accurate interconnect model to reduce the crosstalk effect. The solution for the proposed work is given below

4.1.1 Modeling of RMCB and SMCB Interconnect

In this work, the distribution of CNTs in a bundle is configured using the Gaussian distribution approach for different possible scenarios, as shown in Fig. 1. The total number of CNTs (N_{CNT}) with varying diameters in a bundle can be obtained depending on the bundle width (w =16 nm) and thickness (t = 36 nm). The three different topologies of the SMCB interconnect is depicted in Fig. 1. In the case of SMCB-I, II and III, the different diameters ranges from 1.68 to 7.8 nm are placed in a bundle.

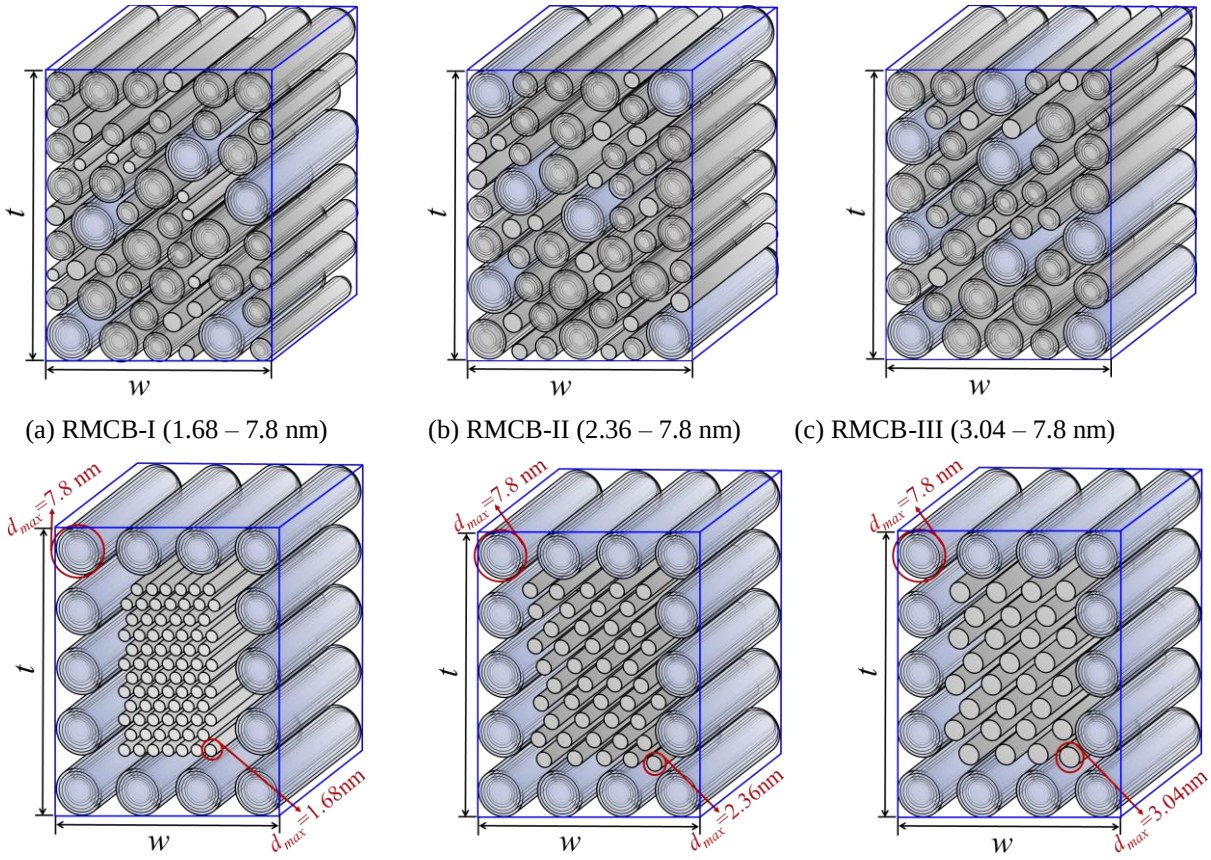

(a) RMCB-I (1.68 – 7.8 nm) (b) RMCB-II (2.36 – 7.8 nm) (c) RMCB-III (3.04 – 7.8 nm)

(d) SMCB-I (1.68 & 7.8 nm) (e) SMCB-II (2.36 & 7.8 nm) (f) SMCB-III (3.04 & 7.8 nm)

Fig. 1. Different configuration of RMCB and SMCB interconnects.

[1] V. R. Kumbhare, P. P. Paltani, and M. K. Majumder, "Performance Analysis of Mixed CNT Bundle Interconnects at 10 nm Technology," *IET Circuits, Devices & Systems*, vol. 14, no. 7, pp. 1049 – 1057, 2020.

Using a fixed bundle area 16 × 36 nm^2 at 10 nm technology, the higher diameter of 7.8 nm is placed at the periphery and the diameter of different CNTs having d_{max} = 1.68, 2.36, and 3.04 nm is placed at the core for SMCB-I, II, and III, respectively. The number of CNTs in a bundle for a spatial arrangement is considered based on the higher tube density of 3.65×10^{12}, 2.43×10^{12}, and 1.91×10^{12} for SMCB-I, II and III, respectively, as shown in Table 1.

Similarly, the random distribution of CNTs in a bundle is carried out for the RMCB-I, II, and III configurations having a mean diameter of 4.74, 5.08, 5.42, and standard deviation of 1.9531, 1.7558, 1.558, respectively. Additionally, each configuration consists of different diameter $d_1 \leq d_i \leq d_{max}$ ranges from 1.68 – 7.8 nm, 2.36 – 7.8 nm, and 3.04 – 7.8 nm for RMCB-I, II, and III, respectively. Using a fixed bundle area of (16 nm × 36 nm), each RMCB exhibits few possible configurations (C-I, C-II, C-III, and C-IV) as shown in Table 2. Irrespective of several possibilities, this work considers a suitable configuration based on the higher tube density. In order to utilize the maximum area of the bundle, the densely packed scenario is considered to have a higher tube density of 5.6×10^{12}, 5.03×10^{12}, and 4.5×10^{12} tubes/cm^2 for RMCB-I, RMCB-II, and RMCB-II, respectively as obtained in Table 2.

Table 1 Distribution of CNT in SMCB Configurations

MCB Type	Distribution of CNTs of diameter d_j in a bundle area of (16 ×36 nm^2) at		Tube density (tubes/cm^2)
	Core	Periphery	
SMCB-I	$d_{1.68}$ = 13	$d_{7.8}$ = 8	3.65×10^{12}
SMCB-II	$d_{2.36}$ = 6	$d_{7.8}$ = 8	2.43×10^{12}
SMCB-III	$d_{3.04}$ = 3	$d_{7.8}$ = 8	1.91×10^{12}

Table 2 Different possible configurations of RMCB-I, II, and III

d_j (nm)	Area (nm^2) required for d_j	Distribution of CNTs in a bundle area of (16 nm×36 nm) using the Gaussian distribution for the three best possible configurations out of several cases in each RMCB											
		RMCB-I (1.68 – 7.8 nm)				RMCB-II (2.36 – 7.8 nm)				RMCB-III (3.04 – 7.8 nm)			
		C-I	C-II	C-III	C-IV	C-I	C-II	C-III	C-IV	C-I	C-II	C-III	C-IV
1.68	3.20	0	0	0	3								
2.36	5.72	2	0	0	3	0	0	0	3				
3.04	8.97	2	2	0	4	2	0	0	4	0	0	*	2
3.72	12.94	4	3	2	4	3	4	0	4	2	0	*	4
4.4	17.64	6	9	12	6	5	5	7	5	4	4	*	6
5.08	23.06	6	9	12	6	6	7	12	7	5	6	*	7
5.76	23.21	4	3	2	2	4	5	7	2	7	9	*	3
6.44	36.08	2	2	0	2	3	4	0	2	3	4	*	2
7.12	43.68	2	0	0	1	2	0	0	1	2	0	*	1
7.8	52.01	0	0	0	1	0	0	0	1	0	0	*	1
Total no. of CNTs		28	28	28	32	25	25	26	29	23	23		26
Tube density (tubes/cm^2)		4.9 ×10^{12}	4.9 ×10^{12}	4.9 ×10^{12}	5.6 ×10^{12}	4.34 ×10^{12}	4.34 ×10^{12}	4.51 ×10^{12}	5.03 ×10^{12}	3.99 ×10^{12}	3.99 ×10^{12}	*	4.5 ×10^{12}

* denotes that invalid configuration that does not follow Gaussian distribution at the particular diameter range

The next subsection presents the performance analysis of different configurations of SMCB and RMCB based interconnects using an active shielding approach.

4.1.2 Performance Analysis of shielded SMCB and RMCB Interconnects

This sub-section presents the worst-case delay of SMCB and realistic RMCB for unshielded and active shielded techniques. In order to reduce the Miller's effect for out-of-phase switching transition, an active shielded line is placed between the coupled interconnects. The crosstalk effect on coupled lines is investigated for dynamic input pulse switching scenarios. Based on the switching on the coupled lines, the inputs to interconnect can be in-phase and out-of-phase to investigate in-phase delay and worst-case delay, respectively [20, 31, 32]. The results indicate that the worst-case delay occurs when the aggressor line switches from low to high and the victim line switches from high to low transitions. In Fig. 2, the results indicate that the shielded RMCB outperforms the shielded SMCB and unshielded RMCB/SMCB configuration in terms of worst-case delay using resistive and CNTFET drivers. The worst-case delay of CNTFET driver-based shielded RMCB and SMCB configuration outperformed by an average of 96.34% and 95.24% compared to unshielded RMCB and SMCB configuration, respectively at 700 µm interconnect length as observed in Figs. 2(a) and 2(b). The primary reason behind the improved performance is due to a lower coupling capacitance between the coupled lines. It is due to the fact that the average diameter (d_{avg}) of a bundle primarily depends on the number of CNTs with different shell dimensions. The wide range of CNTs with different shell dimensions in RMCB primarily reduces the d_{avg} in comparison to the SMCB configurations.

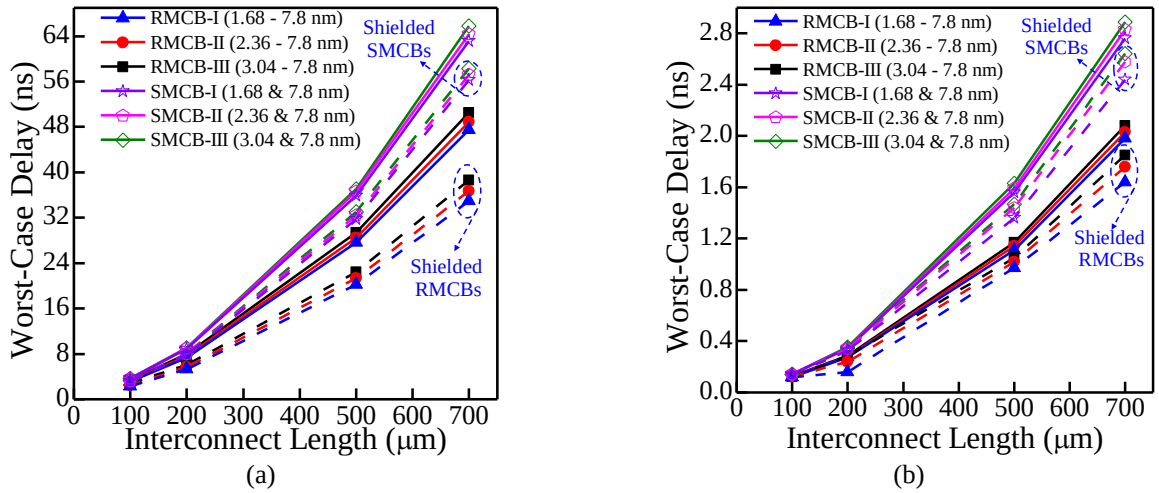

Fig. 2. Worst-case delay of shielded and unshielded RMCB and SMCB interconnect for (a) resistive driver and (b) CNTFET driver

The CNTFET driven shielded RMCB-I provides an improved crosstalk delay of 6.8%, 11.35%, and 32.78%, 36.43%, 37.88% compared to a CNTFET based shielded RMCB-II, III and SMCB-I, II, III, respectively. The voltage drop across the resistive component is primarily the major component of large power dissipation. Higher the resistance of interconnect dissipates large power across it in the form of heat that results in lower interconnect performance. Additionally, power dissipation also depends on the number of tubes in a bundle and the diameter of CNTs. The result of power dissipation obtained for the proposed MCB interconnect is correlated with the simulation result obtained by the other authors in [19] and [20] in Table 3. It is observed that the proposed model outperformed by 99.55% and 44.37% in terms of power dissipation as compared to the other research works given in [19] and [20], respectively.

Table 3. The power dissipation of the proposed work correlates with the existing work in [19] and [20], respectively.

Interconnect Length	Power dissipation (μW) in			
	Khezeli *et al.* [19]		Hamedani *et al.* [20]	Proposed Work
	Copper	Active shielded MWCNT Bundle	Active shielded MWCNT Bundle	RMCB-I
200 μm	294.52	291.53	0.2832	0.6829
400 μm	315.41	296.62	1.23	0.8029
600 μm	346.28	304.95	2.418	1.345
800 μm	379.47	318.80	-	2.144

Although the fabrication has been progressed for a similar diameter of CNTs in a bundle, but the production of high-quality of CNTs is still a challenging task. Therefore, this research work considered the randomly distributed MCB to provide improvement in the performance by adopting a higher tube density of different diameters for future research in VLSI interconnect.

The analysis has been further extended for the propagation delay and equivalent area while considering the identical structure of MWCNT bundle and MLGNR interconnects in the next subsection to counter the inaccurate modeling of interconnects.

4.2 Modeling of Identical Structure of Bundled MWCNT and MLGNR Interconnects[2]

The existing works [20, 33, 34] considered non-identical structural modeling that exhibits inaccurate interconnect performance leading to lower reliability and functionality of ICs. This work is extended to analyze the propagation delay and equivalent area using an accurate identical structure of the MWCNT bundle and MLGNR interconnects. Further, the equivalent parasitic expressions are validated to demonstrate a good agreement between the experimental data and the proposed interconnect model. In this regard, the subsequent subsection provides a suitable solution to counter the non-identical structure model.

4.2.1 Interconnect Modeling for Identical Structures

In this subsection, the physical parameters are accurately considered to design an identical structure of MLWCNT bundle and MLGNR using ITRS benchmark as depicted in Fig. 3 [35]. The physical parameters associated with the MLGNR and Bundled MWCNTs are used as the width/diameter (w = 32 nm, d_{iaN} = 7.12 nm, d_{ia1}= 1 nm), thickness (t = 32 nm), Fermi energy E_F = 0.6 eV, dielectric constant ε_r = 2.2, and interlayer spacing between layers/shells δ= 0.34 nm, etc., at 22 nm technology nodes. The driver-interconnect–load (DIL) setup is used to obtain an equivalent delay of edged MLGNR. The interconnect line in DIL primarily signifies the equivalent electrical model of bundled MWCNT and MLGNR. Industry-

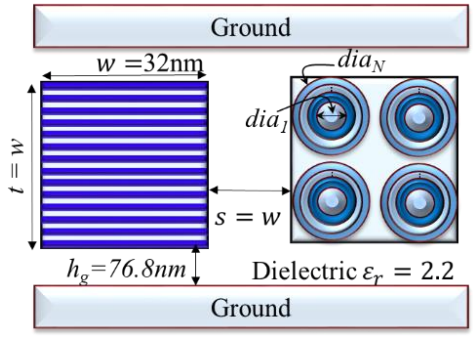

Fig. 3 Cross-sectional view of MLGNR/bundled MWCNT interconnect based on ITRS.

[2] V. R. Kumbhare, P. P. Paltani, C. Venkataiah, and M. K. Majumder, "Analytical study of bundled MWCNT and edged-MLGNR interconnects: Impact on propagation delay and area," *IEEE Transactions on Nanotechnology Letters*, vol. 18, no. 1, pp. 606-610, 2019.

standard HSPICE simulation is carried out to obtain the equivalent delay, which is further validated against the analytical FDTD approach. The proposed ESC models of MLGNR and bundled MWCNT is validated using HSPICE simulations against a highly accurate FDTD technique. Additionally, the scattering resistance agrees to the experimental data with an average deviation of only 5.59% and 9.93% at local and global interconnects, respectively.

4.2.2. Performance Analysis

This sub-section presents a real-time simulation-based approach to compare the performance of edged MLGNR and bundled MWCNT. Using the DIL setup of an edged MLGNR at 22 nm technology, an equivalent delay is obtained for a different number of MWCNTs (with N_{shell} = 10) in a densely packed bundle as depicted in Fig. 4 (a). It is perceived that for a fixed number of MLGNR layers (N_{layer} = 95) at 22nm technology, the number of MWCNTs in a bundle significantly increases for longer interconnects. It is due to the impact of resistive and capacitive parasitics that primarily dominates the overall delay of an interconnect line. Hence, on an average, a rough-edged MLGNR illustrates 44.5% lesser delay compared to a bundled MWCNT for global interconnect lengths.

In order to demonstrate the accuracy, the real-time simulation model is compared with the analytical FDTD based DIL of bundled MWCNT, as shown in Fig. 4 (b). The propagation delay obtained through the proposed FDTD model differs by 2.75% for fewer MWCNTs (N_{MWCNT} = 105) in a densely packed bundle. The proposed analytical model also demonstrates its accuracy with the simulation results by 1.97% and 3.53% for local and global interconnects, respectively. As the number of MWCNTs in a densely packed bundle is lesser compared to the number of layers in MLGNR for local interconnects, the MLGNR consumes 30.17% more area compared to a bundled MWCNT interconnect. However, the area requirement is increased by 97.98% for an MWCNT bundle in comparison to an edged MLGNR for global interconnects. Therefore, a rough-edged MLGNR can outperform a bundled MWCNT with more number of shells for longer interconnects. Moreover, the production of MLGNR is more straightforward than an MWCNT bundle as per the requirement by recent fabrication houses [4, 7, 8]. Hence, a rough-edged MLGNR can be treated as the most promising interconnect material than the MWCNT bundle in terms of fabrication and performance at global interconnect.

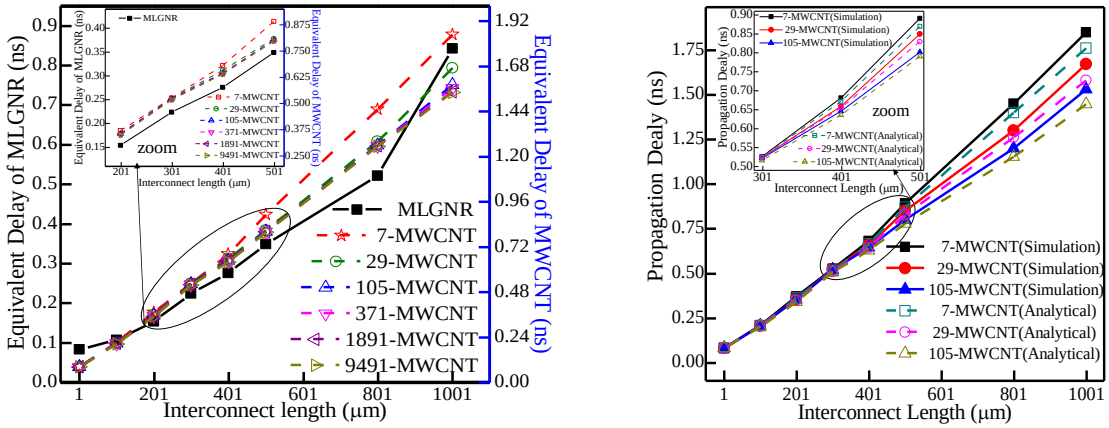

(a) (b)

Fig. 4. The propagation delay of (a) an edged MLGNR and bundled MWCNT for an equivalent delay, and (b) bundled MWCNT (for N_{MWCNT} = 7, 29, 105) using analytical and simulation-based models at different length, respectively.

Further, the work is extended in the subsequent subsection to overcome the challenges associated with the advancement of technology and closer proximity of wire that leads to digital logic faults and lower reliability of the system.

4.3 Contact types and shielding approach on MLGNR based Interconnect[3]

In recent, technology advancement results in higher interconnect density that degrades the interconnect performance and malfunctions the logic operations due to cross-coupling capacitance. To alleviate the crosstalk effect and improve the reliability of system, shielding techniques are required to explore using MLGNR interconnects along with the impact of contact types such as TC and SC. The solution is presented in the following subsection while introducing the impact of TC and SC shielded MLGNR.

4.3.1 Modeling of Top and Side Contact Interconnect

In this section, two different types of contact formation are demonstrated for shielded (active and passive) MLGNR based interconnect geometry, as shown in Fig. 5. Using an active shielding approach, the crosstalk-induced delay can be improved by reducing the effective coupling capacitance as compared to the non-switching passive shielding design. In this regard, the performance of shielded TC-and SC-MLGNR is investigated by considering their equivalent *RLC* model, while considering an accurate physical parameter such as interconnect width (w = 48 nm), thickness (t =115.2 nm), and dielectric constant (ε_r = 2.3) based on the ITRS 2013 [34]. Further, the passive or active shielded MLGNR is positioned between coupled TC/SC-MLGNRs with spacing s. In order to investigate the performance, the shielded TC-and SC-MLGNR are positioned above the ground surface, having a distance h_g = 110.4 nm [35]. The proposed work considered the capacitive loading C_L = 0.28fF at the aggressor and victim lines, while the middle line just acts as a shielding line (active or passive shield) without any loading conditions and accurately considered based on the previously published research article [19]. In the passive shielding scenario, the ground line (GND) or power line (V_{DD}) is placed between the coupled interconnects. However, in an active shielding scenario, the shielded and victim lines are triggered simultaneously with the identical input waveform, while the aggressor line is switched with the opposite input waveform. Therefore, the effective coupling capacitance between the victim and aggressor line reduces due to Miller's Capacitive Factor (MCF). In order to ensure that the victim line and active shielded line having identical switching transitions (either in-phase or out-phase), the

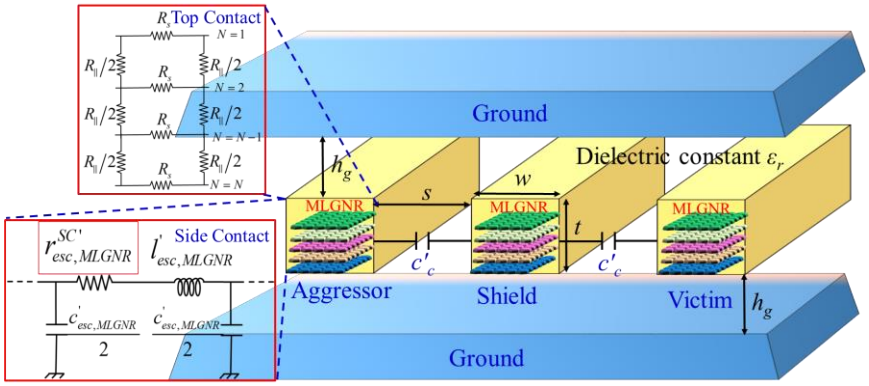

Fig. 5. Shielded MLGNR interconnects geometry based on ITRS 2013.

[3] V. R. Kumbhare, P. P. Paltani, and M. K. Majumder, "Analysis of Top- and Side-Contact MLGNR Interconnects: Impact on Crosstalk, Stability and Electromigration," *Journal of Computational Electronics, Springer*, vol. 19, no. 4, pp. 1588-1596, 2020

parasitic elements of the active shielded line must be similar as the victim line [19, 36].

The quantitative values of equivalent scattering resistance $r'_{esc,MLGNR}$ (TC and SC denoted as $r^{TC'}_{esc,MLGNR}$ and $r^{SC'}_{esc,MLGNR}$, respectively) is obtained accurately for TC and SC-MLGNR as mentioned in Fig. 5 in per unit length (*p.u.l.*) as [1]

$$r^{SC'}_{esc,MLGNR} = \frac{(h/2e^2)}{N^{MLGNR}_{layer} N^{CH}_{MLGNR} \lambda_{eff}} \tag{1}$$

$$r^{TC'}_{esc,MLGNR} = \left[R_s^{-1} + \left(R_{\|} + R_{N-1} \right)^{-1} \right]^{-1} \tag{2}$$

whereas $R_s = h \times \left(2e^2 N^{CH}_{MLGNR} \lambda_{eff}\right)^{-1}$ and $R_{\|} = \rho_{c-axis} \delta_{GNR} / W_{GNR} L$ denote the series and parallel resistances in the case of TC-MLGNR interconnect. The $\rho_{c\text{-}axis}$, h, e, L, and λ_{eff} are referred as c-axis resistivity reported in [20, 25, 28], the Planck's constant, charge of an electron, interconnect length, and MFP based on AsF_5 material edge roughness, respectively. Moreover, the TC-and SC-MLGNR interconnects also exhibit an equivalent inductance ($l'_{esc,MLGNR}$) that consists of kinetic ($l^{SC/TC'}_{k,esc}$) and magnetic ($l^{SC/TC'}_{e,esc}$) inductances. Moreover, the equivalent capacitance ($c'_{esc,MLGNR}$) can be represented as the sum of the charge stored in each layer, and between the nethermost layer and surface plane of graphene gives rise to equivalent quantum ($c'_{q,esc}$) and electrostatic ($c'_{e,esc}$) capacitances, respectively. Using these expressions, the next subsequent subsection demonstrates the crosstalk analysis of TC and SC- MLGNR interconnects at different lengths.

4.3.2 Crosstalk Analysis of TC- and SC-MLGNR

In the proposed work, the DIL setup is used by incorporating the shielding methodology to reduce the impact of coupling capacitance at 32 nm technology. The coupling capacitance between the lines is primarily responsible for the degradation in the performance. When opposite switching is applied at the aggressor and victim lines, the capacitive load experiences a higher delay due to an increase in the coupling capacitance. Whereas, in the case of in-phase switching at the aggressor and victim lines, the capacitive load experiences lower delay compared to the out-phase switching due to the negligible impact of coupling capacitance. Therefore, the crosstalk effect becomes critical with lower dimensions due to the closer proximity of wire that leads to higher coupling capacitance. The coupling capacitance of the interconnect line is obtained using the expression provided in [20, 36]. The improvement in the crosstalk-induced delay for SC-MLGNR is observed than TC-MLGNR as depicted in Fig. 6(a). The performance improvement is mainly due to the number of conducting channels associated with each layer of graphene that leads to lower resistance as compared to TC-MLGNR as described in [25, 26]. Similarly, the delay under the influence of crosstalk becomes more prominent due to an increase in *p.u.l.* interconnect parasitic values. For local and global lengths, the active shielded SC-MLGNR outperforms the TC-MLGNR by 61.21% and 96.21% for spacing s = 5 nm and 57.51% and 95.74% for s = 20 nm, respectively, as shown in Fig. 6(a). Further, the power consumption during switching activities is also investigated in terms of power delay product (PDP) as depicted in Fig. 6(b). Moreover, the SC-based active shielding exhibits 84.80% and 96.82% improved PDP as compared to TC based active MLGNR for spacing s = 5 nm at 1000 µm length. Furthermore, at 32 nm or lower technology, the unintentional peak noise significantly affects the system when the aggressor switches with the input signal and the victim wire remains ideal.

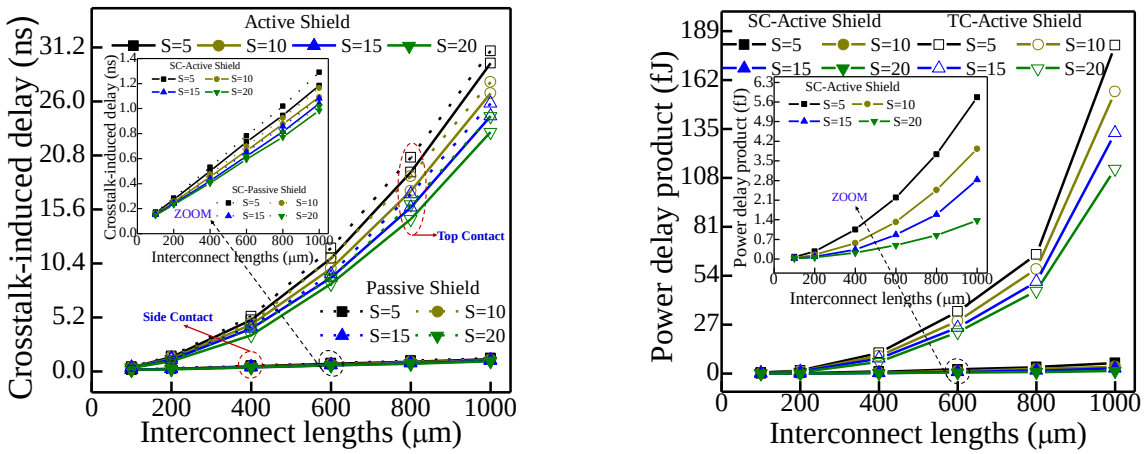

(a) (b)

Fig. 6 (a) The crosstalk-induced delay for shielded TC-and SC-MLGNR (b) PDP of active shielded TC- and SC-MLGNR for different interconnect spacing (in nm).

Therefore, in the current research world, an active shielded SC-MLGNR can be treated as a suitable choice as compared to TC-MLGNR for next-generation interconnect applications. In the subsequent point, the significance of intercalated doping and edge passivation is explored for zig-zag MLGNR to enhance the electronic properties of pristine graphene.

4.4 Performance analysis of intercalated doped zzMLGNR interconnect[4]

In recent years, the demand for high-quality materials and improved performance motivates the research community to improve the transmission of graphene using different intercalated doped materials. The use of intercalation doping primarily prevents the interlayer loss of signal from the edge region and improves the transmission of the signal. The pristine graphene is not yet satisfactory to meet the current demand of lower technology. The optimization and structural investigation are still major scopes to improve the quality of graphene. In this regard, atomic-level structural modification can be a suitable choice to manipulate the structure of pristine graphene while incorporating the doping materials. The impact of doping and edge passivation is required to further explore the improvement in the electronic properties of SC zzMLGNR. In this regard, the next subsection provides a solution to improve the transmission of a signal through the channel region at lower physical dimensions.

4.4.1 Proposed Structure

In the proposed X-zzMLGNR-X Structure (X defined the edge passivation using H and Ru atoms), firstly, carbon to carbon bond length of a_0 =1.42 Å is considered for 8 atom wide (w = 10.01 to 11.21 Å) along B-axes [29]. The H and Ru passivation is used in the zzMLGNR structure as depicted in Fig. 7(a). The number of layers (N_{layer}) for all the configurations is considered as N_{layer} = 4, wherein each layer is separated with different interlayer spacing (δ) along A-axes. The interlayer spacing for pristine, Li, AsF_5, $FeCl_3$, and $MoCl_5$ are considered as 3.4, 3.7, 5.75, 3.94, and 9.2 Å, respectively [27-29]. Further, the doping material is carefully placed manually based on the bonding interaction between the carbon atoms and doping atoms while maintaining the interlayer spacing. Based on the interlayer spacing, various structures are designed while passivating the edge of graphene with H and Ru as depicted in Fig. 7(a). Further, the central channel

[4] V. R. Kumbhare, P. P. Paltani, and M. K. Majumder, "First Principal Analysis of Intercalated Doped Zigzag MLGNR: Prospects for Nano-interconnect Applications," IEEE Transactions on Nanotechnology. (Under Review)

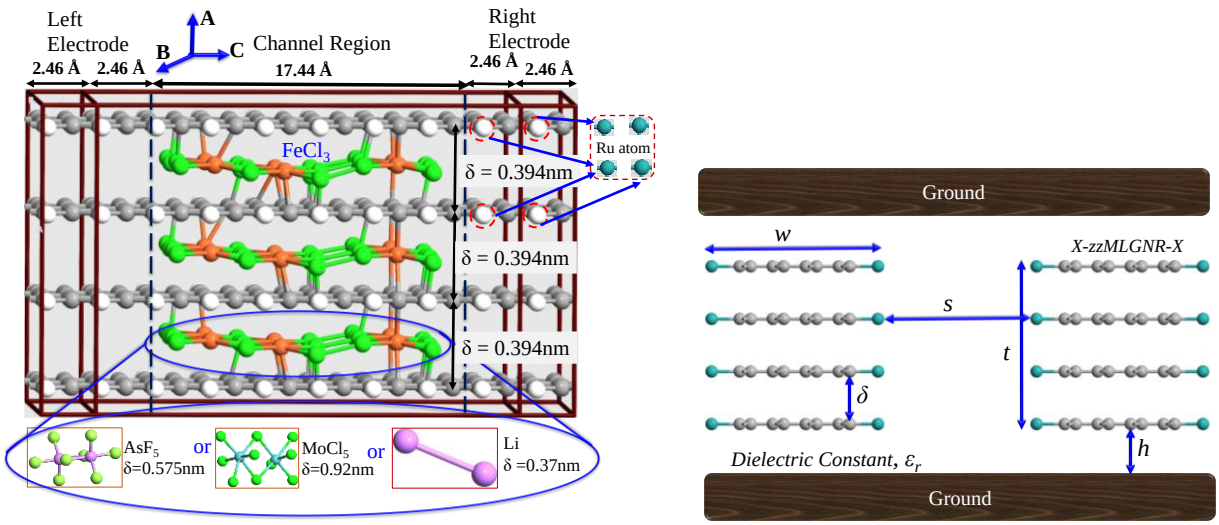

(a) (b)

Fig. 7. (a) Structure of different intercalation doped X-zzMLGNR-X and (b) Cross-sectional view of X-zzMLGNR-X

region is extended along the direction of propagation (i.e., C-axes). After the formation of the structure, the device configuration is divided into three regions such as a left electrode, right electrode, and central channel region. The transformation can be carried out for zig-zag structures having equal left and right periodic electrode lengths of 2.46Å for doped and pristine MLGNR. The central channel region is attached between both left and right electrodes wherein the charge carriers travel due to change in the physical and chemical phenomenon in the central region. The central channel region is primarily responsible for the functionality of the overall design. Using these arrangements, the interconnect modeling is described in the following subsections.

4.4.2 Modeling and Analysis of Interconnect

The equivalent electrical model of X-zzMLGNR-X is demonstrated based on the interconnect geometry as depicted in Fig. 7(b). The physical dimensions such as interconnect width ($w \approx 1$ nm), thickness ($t = 2$ *nm*), height from the ground surface (h_g = 2 nm), and dielectric constant (ε_r = 1.87) are accurately considered [35]. The thickness (t) of interconnect varies in the range of 10.20 Å to 27.60 Å based on the interlayer spacing of pristine/doped material. A novel *pi*-type *RLC* network is used to model the proposed X-zzMLGNR-X structure that provides improved performance as compared to the *L*-type network. Using industry-standard circuit simulator HSPICE, the propagation delay is obtained for pristine and intercalated doped X-zzMLGNR-X interconnects. A comparative investigation is demonstrated between H-zzMLGNR-H and Ru-zzMLGNR-Ru based on the physical dimensions and parameters associated with the interconnects as depicted in Fig. 8. It is evident that the presence of intercalation doped material improves the performance compared to pristine X-zzMLGNR-X due to an increase in the charge carriers in the channel region. It is perceived that both the edge passivated Ru atom provides a significant improvement of propagation delay compared to the H-passivation on both edges of zzMLGNR for an interconnect length ranging from 2 to 12 μm. It is observed that for longer interconnects, the delay increases due to *p.u.l.* increase in the interconnect parasitics associated with zzMLGNR. The results in Fig. 8 depict that the delay of Li doped Ru-zzMLGNR-Ru is outperformed by 43.98%, 51.26%, 72.30%, and 74.76% at 2μm length, whereas 47.03%, 54.75%, 75.63%, and 83.99% at 12 μm length as compared to $FeCl_3$, AsF_5, $MoCl_5$, and

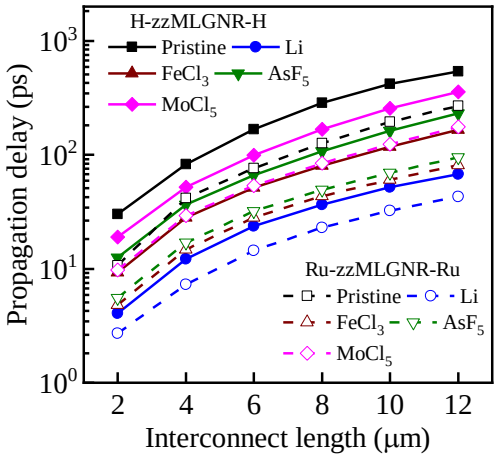

Fig. 8. A comparative investigation of propagation delay for pristine and different intercalated doped H-zzMLGNR-H and Ru-zzMLGNR-Ru interconnect.

pristine Ru-zzMLGNR-Ru interconnect, respectively. The delay performance of Li doped Ru-zzMLGNR-Ru is improved at global lengths due to an increase in conductivity, electron mobility, and reduction of intershell electron hoping. From device physics, it is evident that the conductivity is directly proportional to the mobility of the electrons in the channel region that is primarily the reason behind a higher signal transmission. However, the reduction in intershell electron hopping is observed due to a smaller interlayer spacing in the presence of intercalated doped materials, as observed from Fig. 8. Moreover, the proposed structure is compared with the state-of-the-art techniques summarized in Table 4.

Table 4. The proposed structure is compared with the existing state-of-the-art.

Features	Nishad *et al.* [21]	T. Kaur *et al.* [22]	M. Kaur *et al.* [23]	Nishad *et al.* [29]	Xu *et al.* [30]	Proposed Design
Structure Optimization	Thickness	No	No	Yes	No	Yes
Materials	MLGNR	MLGNR, MCB and Cu	zzMLGNR	AGNR	MLGNR	zzMLGNR
Edge Passivation	Rough Edge	No	No	Pd, Pt, Rh, and Ru	No	H and Ru
Intercalated doped materials	Li and AsF_5	AsF_5	AsF_5 and Li	No	High-k dielectric	Li, $FeCl_3$, $MoCl_5$, and AsF_5
Parameter extraction	No	No	No	Yes	No	Yes
N_{layer}	36	96	Not mentioned	1	Not mentioned	4
N_{ch}	Not mentioned	Not mentioned	Not mentioned	8	Not mentioned	28
Physical Dimensions	w= 6nm, s=6nm, t=13.2nm, h_g=13.2nm and ε_r=1.87	w=24, A/R=2.34, h_g=56nm, ε_r=2.48	w=24, A/R=2.34, h_g=56nm, ε_r=2.48	w=1nm, s=1nm, h_g =2nm, ε_r=1.87	w=11.5nm, t=26.91nm, h_g=17.25nm, ε_r=200 (SrTiO3)	w=1nm, s=1nm, h_g=2nm, ε_r=1.87
Analysis	Delay, Energy Delay Product (EDP)	Delay, power dissipation and PDP	Delay, Bandwidth, and skin depth	Delay, transmission spectrum, EDP	Delay, Bandwidth	Delay, transmission, and Band structure
Transmission spectrum	No	No	No	9	No	18.76
Delay Performance	22.9ps	151ps	27.55ps	119 ps	4.568 ns for pristine and 0.848 ns for $SrTiO_3$	2.7 ps for Li doped

It can be observed that the proposed design possesses lesser delay at lower technology dimensions. It is due to the fact that the Li as intercalated doped material in Ru-zzMLGNR-Ru increases the charge carriers in the channel region. Therefore, it exhibits more number of conducting channels (N_{ch}) resulting in lower scattering resistance and higher quantum capacitance. However, the cumulative effect of both the resistance and capacitance possess a lesser delay in comparison to the other existing methodologies [21-23, 29, 30]. Therefore, it is concluded that both edges of zzMLGNR terminated with Ru atoms under the influence of Li intercalated doped material is significantly improved the performance. Hence, it can be considered as an emerging choice for next-generation nano-interconnect applications.

5. Conclusions and Future Work

The complete work presented in the thesis demonstrates the significance of graphene based interconnects to address the challenges associated with interconnects at advanced technology nodes. A comprehensive literature analysis unveils several issues that degrade the performance, reliability, and functionality of interconnects. Initially, the first phase of the work demonstrates an accurate modeling of realistic RMCB and SMCB interconnects using high tube density at lower physical dimensions. Based on the analysis and investigation, it can be inferred that the realistic active shielded RMCB demonstrates improved performance as compared to unshielded and shielded SMCBs. It is perceived that the worst-case delay of CNTFET based shielded RMCB-I provides 19.17%, 35.69%, and 41.96% improved performance than unshielded RMCBs, shielded SMCBs, and unshielded SMCBs configuration, respectively.

In the second phase of the work, a comparative analysis of propagation delay and area for rough-edged MLGNR and MWCNT bundled interconnects is demonstrated based on the analytical FDTD and industry-standard simulation approach. The proposed equivalent model is in good agreement with the MTL in terms of delay. It is observed that the model expressions exhibit a good agreement with experimental data with an average deviation of below 9.93%. Furthermore, the equivalent delay is validated against the analytical FDTD approach that differs from the real-time simulation results only by 1.97% and 3.53% for local and global interconnects, respectively. Additionally, it is observed that the time complexity involved in simulation is lesser by 66.57% and 83.68% in comparison to FDTD at 100 and 1000 μm, respectively. Furthermore, the area requirement for rough-edged MLGNR is 97.98% lesser compared to bundled MWCNT at global interconnect lengths.

In the third phase of the work, the significance of shielding and contact types is demonstrated due to the closer proximity of wire that results in improper functionality and digital logic faults at lower dimensions. This work considers SC and TC MLGNR interconnects to demonstrate stability and crosstalk reliability issues at global lengths. Using an accurate and efficient *pi*-type equivalent electrical model, the active shielded SC-MLGNR provides improved performance (crosstalk-induced delay) by 59.36% and 95.97% than TC-MLGNR at local and global lengths, respectively. Further, the analysis is carried out for PDP that exhibits 84.80% and 96.82% improvement for active shielded SC-MLGNR as compared to the TC-MLGNR for the spacing of 5 nm at l00 and 1000μm lengths, respectively. Encouragingly, it is observed that an active shielded SC-MLGNR possesses an average of 45.87% improved peak noise in comparison to a TC-MLGNR to address the digital logic faults efficiently.

Apart from this, the work is further extended to improve the performance of the SC-MLGNR interconnects. This is accomplished by using a suitable interlayer doping that enhances the current carrying capability, improves the transmission of signal, and provides a large number of conducting channels compared to the pristine graphene. The performance in terms of propagation delay is carried out for pristine

and intercalated doped materials such as Li, AsF_5, $FeCl_3$, and $MoCl_5$ X-zzMLGNR-X interconnects. It is also observed that both edges of zzMLGNR terminated with Ru atom under the influence of Li intercalated doped material provides 83.99% improved performance compared to pristine structures at higher lengths. Therefore, it has been concluded based on the entire work that the Li doped zz-MLGNR under ruthenium edge passivation can be considered as a suitable choice for interconnect application in cutting-edge technology.

Depending on the above remarks, this work primarily presents an in-depth analysis in the field of nano-interconnect that can provide a different direction to the readers and research communities. Several methodologies have been presented to counter the challenges with the lower physical dimensions in order to fulfill the current demand for cutting-edge technology. However, there are still several challenges associated with the graphene-based interconnect that need to resolve for wide-scale deployment. This work can be extended to overcome the challenges related to the metal-graphene interface while considering the contact materials having higher work functions. This can be achieved by improving the different contact materials while performing the atomic-level simulation. Further, the work can provide the future direction to understand the growth process and diameter control of nanotubes in a bundle. The highly aligned and densely packed carbon nanotubes are required to investigate under a wide range of growth parameters. Apart from this, the work can be extended once the fabrication lines up to control the chirality and edge roughness of CNT and GNR, respectively. Moreover, there are still several challenges associated with the growth of graphene and pattering. In order to overcome these challenges, it is highly recommended to used ultra-high-resolution lithography to avoid roughness issues below 5 nm technology. Using ultra-high-resolution electron lithography, the width of graphene can be narrow down with a smooth edges resulting in better performance due to less edge scattering.

Organization of Thesis

This thesis is divided into seven chapters to attain the solution to the challenges defined in the problem statement. The introduction of each chapter is presented at the beginning and a summary of the chapter related to the concern problem is presented at the end of each chapter. A brief outlines of each chapter is given below

Chapter 1 introduces the significance of on-chip and off-chip interconnects along with the evolution of different interconnect materials. Further, the challenges associated with each technology are presented. Besides, the significance of CNT and GNR is presented that is thrust for the research while considering graphene as an emerging material for interconnect application to overcome the specific challenges for the purpose of current research work.

Chapter 2 presents the diverse structure of graphene and its unique properties together with the fabrication aspects in the recent era. Further, different methodologies for synthesis and growth of CNT and GNR is explored along with the fabrication aspects for interconnect applications. Based on the extensive literature survey, the different modeling schemes such as luttinger liquit model, diameter dependent model, MCB model, MLGNR model etc., are presented for interconnect application. The literature review particularly focuses on existing CNT and GNR based interconnects and their associated challenges. Further, several technical gaps are identified based on state-of-the-art research.

Chapter 3 emphasized a realistic methodology to model the RMCB and SMCB structures based on higher tube density. Further, the different configurations of RMCB and SMCB structures are modeled into a *pi*-type electrical network. Using DIL setup, the interconnect performance is measured based on the

propagation delay, crosstalk-induced delay, and power dissipation for different interconnect lengths. Further, a comparative analysis of the proposed work is demonstrated with the CNT based MCB interconnects.

Chapter 4 demonstrates an accurate comparative analysis of the identical structure of the MWCNT bundle and MLGNR interconnects. Further, the proposed structure is modeled into MTL that is further simplified into the ESC model. Accurate modeling of interconnect is demonstrated based on the standard ITRS benchmark physical dimensions. Later, the interconnect parasitics associated with *pi*-type novel electrical circuits are validated using experimental data. Further, based on different numbers of MWCNT in a bundle and MLGNR, an equivalent propagation delay and area are obtained. Furthermore, the highly accurate analytical model is presented based on the FDTD approach that is used to validate the results.

Chapter 5 introduces the significance of the different types of contact formation, such as top and side contacts. Based on the type of contacts, the active and passive shielded MLGNR are accurately modeled to critically analyze the crosstalk reliability of interconnect. Further, an analytical approach based on the ABCD parameter is considered to investigate the relative stability of MLGNR for different lengths.

Chapter 6 deals with the atomic level structural analysis to increase the functionality and performance of the pristine graphene. This can be achieved by incorporating the intercalated dielectric material between the graphene layers. Further, the significance of both side edge passivation (H and Ru atoms) is demonstrated to enhance the overall performance of the graphene. Based on the extracted parameter from the optimized structures, efficient modeling of interconnect is demonstrated for pristine and zzMLGNR interconnect under the influence of hydrogen and ruthenium edged passivation to investigate the delay performance.

Chapter 7 describes the conclusion drawn from the entire work and discussed the potential direction for further research.

List of Publications

Published Journals:

1. **V. R. Kumbhare**, R. Kumar, M. K. Majumder, S. Kumar, P. P. Paltani, B. K. Kaushik, and R. Sharma, "High-Speed Interconnects: History, Evolution, and the Road Ahead," in *IEEE Microwave Magazine*. (Accepted, In Press) **(I.F. 2.928)**
2. **V. R. Kumbhare**, P. P. Paltani, and M. K. Majumder, "Performance Analysis of Mixed CNT Bundle Interconnects at 10 nm Technology," in *IET Circuits, Devices & Systems*, vol. 14, no. 7, pp. 1049 – 1057, 2020. **(DOI:**10.1049/iet-cds.2019.0516**)** **(IF. 1.290**)
3. **V. R. Kumbhare**, P. P. Paltani, and M. K. Majumder, "Analysis of Top- and Side-Contact MLGNR Interconnects: Impact on Crosstalk, Stability and Electromigration," in *Journal of Computational Electronics, Springer*, vol. 19, no. 4, pp. 1588-1596**,** 2020.**(DOI:**10.1007/s10825-020-01558-7**)** **(I.F. 1.532)**
4. **V. R. Kumbhare**, P. P. Paltani, and M. K. Majumder, "Relative stability of shielded top- and side contact multi-layered GNR interconnects," in *International Journal of Electronics Letters*, 2020. **(DOI**:10.1080/21681724.2020.1793393**)** **(I.F. 1.2)**
5. **V. R. Kumbhare**, P. P. Paltani, C. Venkataiah, and M. K. Majumder, "Analytical study of bundled MWCNT and edged-MLGNR interconnects: Impact on propagation delay and area," in *IEEE Transactions on Nanotechnology Letters*, vol. 18, no. 1, pp. 606-610, 2019. **(DOI: 10.1109/TNANO.2019.2920679)**. **(IF. 2.857)**
6. **V. R. Kumbhare**, P. P. Paltani, and M. K. Majumder, "Impact of interconnect spacing on crosstalk for multi-layered graphene nanoribbon," in *IETE Journal of Research, Taylors & Francis*, pp. 1-10, 2019 **(DOI: 10.1080/03772063.2019.1637788)** **(I.F. 1.125)**

Communicated Journals:

1. **V. R. Kumbhare**, P. P. Paltani, and M. K. Majumder, "First Principal Analysis of Intercalated Doped Zigzag MLGNR: Prospects for Nano-interconnect Applications," ***IEEE Transactions on Nanotechnology***. (Under Review)

Published Conferences:

1. **V. R. Kumbhare**, P. P. Paltani, and M. K. Majumder, "First Principle Study of Electronics Property of Doped/Undoped Graphene Structure for Interconnect Application," In *Proceedings of 21st IEEE International Conference on Nanotechnology* (**IEEE-NANO 2021**). (Accepted)
2. **V. R. Kumbhare**, P. P. Paltani, and M. K. Majumder, "An efficient method to reduce crosstalk for multi-layered GNR interconnects at 32 nm Technology," In *Proceedings of 19th IEEE International Conference on Nanotechnology* (IEEE-NANO 2019, July 22-26) at The Parsian Macao, Macau SAR, China, pp. 23-27, 2019. **(DOI:**10.1109/NANO46743.2019.8993958.)
3. **V. R. Kumbhare**, P. P. Paltani, and M. K. Majumder, "Novel approach for improved signal integrity and power dissipation using MLGNR interconnects," In *Proceedings of 23rd International Symposium on VLSI Design and Test* (VDAT 2019, July 2-6, 2019) at IIT Indore, India, pp. 617-629, 2019. **(DOI: 10.1007/978-981-32-9767-8_51)**
4. **V. R. Kumbhare**, P. P. Paltani, and M. K. Majumder, "Signal integrity analysis for diameter dependent mixed carbon nanotube bundle interconnects," In: *Tuba M., Akashe S., Joshi A. (eds) Information and Communication Technology for Sustainable Development. Advances in Intelligent Systems and Computing*, vol. 933. Springer, Singapore, vol. 933, pp. 481-489, 2019. **(DOI: 10.1007/978-981-13-7166-0_48)**
5. **V. R. Kumbhare**, P. P. Paltani, and M. K. Majumder, "Future of graphene based interconnect technology - A reality or a distant dream," In *Proceedings of 5th IEEE Uttar Pradesh Section International Conference on Electrical, Electronics and Computer Engineering* (UPCON), Gorakhpur, pp. 1-7, 2018. **(DOI:** 10.1109/UPCON.2018.8596900**)**

Published Book:

1. M. K. Majumder, **V. R. Kumbhare,** A. Japa, and B. K. Kaushik, "*Introduction to Microelectronics to Nanoelectronics: Design and Technology*," 1st edition, Boca Raton, CRC Press, ISBN No. 9780367502379, 24 Nov. 2020.

References

[1] W. Cao *et al*., "2-D Layered Materials for Next-Generation Electronics: Opportunities and Challenges," *IEEE Transactions on Electron Devices*, vol. 65, no. 10, pp. 4109-4121, 2018.

[2] H. Li, C. Xu, N. Srivastava and K. Banerjee, "Carbon Nanomaterials for Next-Generation Interconnects and Passives: Physics, Status, and Prospects," *IEEE Transactions on Electron Devices*, vol. 56, no. 9, pp. 1799-1821, 2009.

[3] A. Upadhyay, A. Kushwaha, P. Rastogi, Y. Chauhan, and S. K. Vishvakarma, "Explicit Model of Channel Charge, Backscattering and Mobility for Graphene FET in Quasi-Ballistic Regime," *IEEE Transactions on Electron Devices*, vol. 65, no. 12, pp. 5468 - 5474, 2018.

[4] W. Liu, H. Li, C. Xu, Y. Khatami, K. Banerjee, "Synthesis of high-quality monolayer and bilayer graphene on copper using chemical vapor deposition", vol.49, no. 13, pp. 4122–4130, 2011.

[5] S. Das, S. Bhattacharya, D. Das, and H. Rahaman, "A survey on pristine and intercalation doped graphene nanoribbon interconnect for future VLSI circuits", *AIMS Materials Science*, vol. 8, no. 2, pp. 247-260, 2021.

[6] D. Das, H. Rahaman, "Analysis of Crosstalk in Single- and Multiwall Carbon Nanotube Interconnects and Its Impact on Gate Oxide Reliability", *IEEE Transactions on Nanotechnology*, vol. 10, no. 6, pp. 1362 – 1370, 2011.

[7] M. K. Majumder, B. K. Kaushik, and S. K. Manhas, "Analysis of delay and dynamic crosstalk in bundled carbon nanotube interconnects", *IEEE Transactions on Electromagnetic Compatibility*, vol. 56, no. 6, pp. 1666-1673, 2014.

[8] S. Subash, J. Kolar, and M. H. Chowdhury, "A new spatially rearranged bundle of mixed carbon nanotubes as VLSI interconnection", *IEEE Transactions on Nanotechnology*, vol. 12, no. 1, pp. 3-12, 2013.

[9] P. J. Burke, "Lüttinger liquid theory as a model of the gigahertz electrical properties of carbon nanotubes," *IEEE Transactions on Nanotechnology*, vol. 1, no. 3, pp. 129–144, 2002.

[10] A. Raychowdhury and K. Roy, "A Circuit Model for Carbon Nanotube Inteconnects: Comparative Study with Cu Interconnects for Scaled Technologies", In *Proceedings of IEEE/ACM International Conference on Computer Aided Design*, pp. 237-240, 2004.

[11] N. Srivastava and K. Banerjee, "Performance analysis of carbon nanotube interconnects for VLSI applications", In *Proceedings of IEEE/ACM International Conference on Computer-Aided Design, (ICCAD-2005)*, San Jose, CA, USA, pp. 383-390, 2005.

[12] A. Nieuwoudt and Y. Massoud, "Understanding the impact of inductance in carbon nanotube bundles for VLSI interconnect using scalable modeling techniques", *IEEE Transactions on Nanotechnology*, vol. 5, no. 6, pp. 758–765, 2006.

[13] A. Naeemi and J. D. Meindl, "Compact physical models for multiwall carbon-nanotube interconnects", *IEEE Electron Device Letters*, vol. 27, no. 5, pp. 338-340, 2006.

[14] S. Haruehanroengra and W. Wang, "Analyzing Conductance of Mixed Carbon-Nanotube Bundles for Interconnect Applications," *IEEE Electron Device Letters*, vol. 28, no. 8, pp. 756-759, 2007.

[15] P. U. Sathyakam and P. S. Mallick, "Transient analysis of mixed carbon nanotube bundle interconnects", *Electronics Letters*, vol.47, no. 20, pp. 1134–1136, 2011.

[16] Y. Khatami, H. Li, C. Xu, and K. Banerjee, "Metal-to-Multilayer-Graphene Contact—Part I: Contact Resistance Modeling", *IEEE Transactions on Electron Devices*, vol. 59, no. 9, pp. 2444-2452, 2012.

[17] Y. Khatami, H. Li, C. Xu and K. Banerjee, "Metal-to-Multilayer-Graphene Contact—Part II: Analysis of Contact Resistance", *IEEE Transactions on Electron Devices*, vol. 59, no. 9, pp. 2453-2460, 2012.
[18] D. W. Yue, C. H. Ra, X. C. Liu, D. Y. Lee, W. J. Yoo, "Edge contacts of graphene formed by using controlled plasma treatment", *Nanoscale* vol. 7, no. 2, pp. 825 – 831, 2015.
[19] M. R. Khezeli, M. H. Moaiyeri, and A. Jalali, "Active Shielding of MWCNT Bundle Interconnects: An Efficient Approach to Cancellation of Crosstalk-Induced Functional Failures in Ternary Logic," *IEEE Transactions on Electromagnetic Compatibility*, vol. 61, no. 1, pp. 100–110, 2019.
[20] S. G. Hamedani and M. H. Moaiyeri, "Comparative Analysis of the Crosstalk Effects in Multilayer Graphene Nanoribbon and MWCNT Interconnects in Sub-10 nm Technologies," *IEEE Transactions on Electromagnetic Compatibility*, vol. 62, no. 2, pp. 561 – 570, 2020.
[21] A. K. Nishad and R. Sharma, "Lithium-Intercalated Graphene Interconnects: Prospects for On-Chip Applications," *IEEE Journal of Electron Device Society*, vol. 4, no. 6, pp. 485-489, 2016.
[22] T. Kaur, M. K. Rai, and R. Khanna, "Effect of temperature on the performance analysis of MLGNR interconnects," *Journal of Computational Electronics*, vol. 18, pp. 722–736, 2019.
[23] M. Kaur *et al.*, "RF analysis of intercalated graphene nanoribbon-based global-level interconnects," *Journal of Computational Electronics*, vol. 19, pp. 1002–1013, 2020.
[24] C. Xu, H. Li, and K. Banerjee, "Modeling, Analysis, and Design of Graphene Nano-Ribbon Interconnects", *IEEE Transactions on Electron Devices*, vol. 56, no. 8, pp. 1567-1578, 2009.
[25] A. K., Nishad and R. Sharma, "Performance Improvement in SC-MLGNRs Interconnects Using Interlayer Dielectric Insertion", *IEEE Transactions on Emerging Topics of in Computing*, vol. 3, no. 4, pp. 470 – 482, 2015.
[26] R. Kumar, R. Dhiman, and R. Chandel, "Performance Analysis of Top-Contact MLGNR Based Interconnects," In Proceedings of *IEEE International Symposium on Nanoelectronic and Information Systems (iNIS)*, Gwalior, pp. 11–16 (2016)
[27] J. Jiang *et al.*, "Intercalation Doped Multilayer-Graphene-Nanoribbons for Next-Generation Interconnects", *Nano Letters*, vol. 17, no. 3, pp. 1482–1488, 2017.
[28] J. Kang *et al.*, "On-chip intercalated-graphene inductors for next-generation radio frequency electronics", *Nature Electron*ics, vol. 1, pp. 46–51, 2018.
[29] V. K. Nishad, A. K. Nishad, B. K. Kaushik, and R. Sharma, "First-Principle Analysis of Transition Metal Edge-Passivated Armchair Graphene Nanoribbons for Nanoscale Interconnects," *IEEE Transactions on Nanotechnology*, vol. 20, pp. 92-98, 2021.
[30] P. Xu and Z. Pan, "Collaborative Applying the Ultra-low-k Dielectric and the High-k Dielectric Materials for Performance Enhancement in Coupled Multilayer Graphene Nanoribbon Interconnects," *IEEE Journal of Electron Devices Society*, vol. 8, pp. 200-212, 2020.
[31] S. Das, S. Bhattacharya, D. Das and H. Rahaman, "Modeling and Analysis of Electro-Thermal Impact of Crosstalk Induced Gate Oxide Reliability in Pristine and Intercalation Doped MLGNR Interconnects", *IEEE Transactions on Device and Materials Reliability*, vol. 19, no. 3, pp. 543-550, 2019.
[32] A. Leong, V. Swamy, and N. Ramakrishnan, "Multilayer graphene electrodes for one-port surface acoustic wave resonator mass sensor", *Japanese Journal of Applied Physics*, vol. 56, no. 2, pp. 024301-1-024301-6, 2017.
[33] M. S. Sarto and A. Tamburrano, "Comparative analysis of TL models for multilayer graphene nanoribbon and multiwall carbon nanotube interconnects," In *Proceedings of IEEE International Symposium on Electromagnetic* Compatibility, Fort Lauderdale, FL, pp. 212-217, 2010.
[34] M. K. Majumder, N. R. Kukkam, and B. K. Kaushik, "Frequency response and bandwidth analysis of multi-layer graphene nanoribbon and multi-walled carbon nanotube interconnects," *IET Micro & Nano Letters*, vol. 9, no. 9, pp. 557-560, 2014.
[35] International Technology Roadmap for Semiconductor (ITRS 2013): [Online], http://www.itrs.net
[36] M. Sahoo, P. Ghosal and H. Rahaman, "Modeling and Analysis of Crosstalk Induced Effects in Multiwalled Carbon Nanotube Bundle Interconnects: An ABCD Parameter-Based Approach," *IEEE Transactions on Nanotechnology*, vol. 14, no. 2, pp. 259-274, 2015.